



Settlement Predictions of a Trial Embankment on Ballina Clay

Shan Huang, Ph.D. candidate, Discipline of Civil, Surveying and Environmental Engineering, The University of Newcastle, Callaghan, NSW 2308, Australia; email: SHuang2@uon.edu.au

Jinsong Huang, Professor, Discipline of Civil, Surveying, and Environmental Engineering, The University of Newcastle, Callaghan, NSW 2308, Australia; email: jinsong.huang@newcastle.edu.au

Richard Kelly, Ph.D., SMEC, Australia & New Zealand Division; email: DrRichard.Kelly@smec.com

Cheng Zeng, Ph.D. candidate, Discipline of Civil, Surveying, and Environmental Engineering, The University of Newcastle, Callaghan, NSW 2308, Australia; email: cheng.zeng@uon.edu.au

Jiawei Xie, Ph.D. candidate, Discipline of Civil, Surveying, and Environmental Engineering, The University of Newcastle, Callaghan, NSW 2308, Australia; email: jiawei.xie@uon.edu.au

ABSTRACT: *An instrumented trial embankment was constructed on the soft ground with the use of prefabricated vertical drains at Ballina in northern New South Wales (NSW, Australia) as part of the Australian Research Council Centre of Excellence for Geotechnical Science and Engineering (CGSE) research program. Comprehensive geotechnical site investigations were performed and field monitoring data were collected, which make it possible to study and compare various settlement prediction methods. In this paper, the Asaoka method, the Hyperbolic method, and the Bayesian updating approach are employed to predict the settlement of the trial embankment. The predictions of the three methods are compared for different amounts of monitoring data. The results show that the predicted settlements are close to the measurements and the accuracy of the ultimate settlement prediction can be improved by incorporating more monitoring data. The time increment can significantly influence the accuracy of the result predicted by the Asaoka method. The Bayesian updating approach is in agreement with the observed settlement by using only 215 days of the monitoring data.*

KEYWORDS: Ballina clay, embankment, settlement prediction, Bayesian updating, back analysis

SITE LOCATION: [Geo-Database](#)

INTRODUCTION

The prediction of settlement for embankment constructed on soft soils is a critically important issue in soil mechanics. This provides the analyst with early confidence in the eventual outcome so that informed decisions can be made.

To study the settlement behavior of soft soils, a full-scale trial embankment with prefabricated vertical drains (PVDs) was constructed at Australia's first National Field Testing Facility (NFTF) for soft soils at Ballina, New South Wales. Many practitioners and academics were invited by the Australian Research Council Centre of Excellence for Geotechnical Science and Engineering (CGSE) to participate in the Embankment Prediction Symposium 2016, and were asked to perform Ballina embankment behavior predictions by different types of analysis, ranging from hand calculation to complicated numerical analyses.

Buttling et al. (2018) predicted the settlement performance by hand calculation carried out in spreadsheet, and they employed a numerical analysis based on a 2D finite element program incorporated in PLAXIS to do comparison analyses with the hand calculations. Lim et al. (2018) carried out the predictions using hand calculation and the finite difference method. Yang and Carter (2018) proposed a Hunter Clay model to characterize the mechanical behavior of the natural soft clay at Ballina and then incorporated this model into the finite strain consolidation theory to do settlement prediction. Based on an elastoviscoplastic anisotropic constitutive model, which is implemented in PLAXIS software, Rezania et al. (2018) carried out numerical settlement predictions.

Submitted: 18 December 2020; Published: 25 October 2021

Reference: Huang S., Huang J., Kelly R., Zeng C., and Xie J. (2021). Settlement Predictions of a Trial Embankment on Ballina Clay. International Journal of Geotechnical Case Histories, Volume 6, Issue 4, pp. 101-114, doi: 10.4417/IJGCH-06-04-07



Müthing et al. (2018) applied a 2D finite element model to simulate the consolidation and creep processes underneath the embankment on soft, estuarine clay and predicted the embankment behavior in terms of transient settlement and pore water pressure dissipation. Tschuchnigg and Schweiger (2018) performed short-term and long-term embankment settlement predictions based on 2D and 3D finite element analyses. Le, Airey, and Surjadinata (2018) used the commercial finite element package ABAQUS and the Modified Cam Clay model available within ABAQUS to perform a plane strain, fully coupled finite element analysis and to predict the behavior of the soft clay. Liu et al. (2018) combined the probabilistic method with the finite element program PLAXIS 2D to illustrate the variability of predicted settlement, horizontal displacement, and pore pressure.

Apart from the methods presented above, many observational methods for settlement prediction of soft soils have also been proposed. The Asaoka method was proposed by Asaoka (1978) and the Hyperbolic method was introduced and refined by Tan (1991) to predict the ultimate settlement and in-situ coefficient of consolidation for one-dimensional consolidation. These two methods are widely applied, as they are simple and easy to use. In addition, the Bayesian approach has been proved to be a rational and robust means of updating the input parameters and accurately predicting the long-term behavior based on reliable observations (Kelly and Huang 2015a; Hsein Juang et al. 2013; Zhang, Tang, and Zhang 2010; Miranda, Correia, and e Sousa 2009; Honjo, Wen-Tsung, and Guha 1994).

In this study, to accurately predict the long-term behavior of the Ballina embankment, the Asaoka, Hyperbolic, and Bayesian methods are all applied. The comparison of the three different methods is also performed to determine their accuracy of predictions compared to actual observations. It was found that the settlement data beyond the 60% consolidation stage is needed in both the Asaoka and Hyperbolic methods to make accurate predictions. The appropriate monitoring duration and supportable data recording interval for field monitoring programs are also suggested to achieve cost-effective outcomes.

BRIEF INTRODUCTION OF THE BALLINA EMBANKMENT

The Ballina embankment was constructed in Ballina, NSW, Australia, to be approximately 80 m long, 16 m wide, and with a fill thickness of 3.0 m. As shown in Fig. 1 (Chan, Poon, and Perera 2018), the soil deposit consists of a surface layer of clayey soil of about 1.3 m thick, and a second layer of soft Ballina clay of about 8.5 m thick. The third layer is a sandy layer or clayey sand layer of about 4.2 m thick. The fourth is a layer of sand with varied thickness. Below the sand layer is a thick stiff clay layer. The detailed description of the soil strata can be found in Kelly et al. (2018).

This embankment was instrumented extensively to measure pore pressure, vertical deformations, and horizontal soil pressure at many key locations over time. The instrumentation included several settlement plates, inclinometers, and magnetic extensometers, total and push in pressure cells, hydrostatic profile gauges, and numerous pore pressure probes. Four settlement plates were installed along the embankment center line at the ground surface prior to construction to record the settlement of the ground surface below the embankment. A total of four inclinometers were installed to measure the lateral displacements. Two magnetic extensometers were installed to measure the vertical displacement of the soil at different depths in the ground. Two hydrostatic pressure gauges (HPG) were installed on either side of different drain types.

The obtained field and laboratory data provided by CGSE were summarized in Pineda et al. (2016). Vertical drains are applied to improve Ballina soft soil by providing a horizontal drainage path along which excess pore water pressures caused by a surcharge can dissipate faster than by a vertical drainage path alone. According to Kelly et al. (2017); Kelly et al. (2018) and Zheng et al. (2018), the PVDs were installed on a 1.2 m square grid with a drain spacing of 1.1 m under the embankment, which is presented in Fig. 2(a), and the buried depth is 14.2 m. The soil zone adjacent to the drain is termed as installing PVDs results in disturbance. The undisturbed zone is around the smear zone, which is presented in Fig. 2(b). The vertical load on the top surface varies with time, and the field settlement monitored in different days, as shown in Fig. 3.

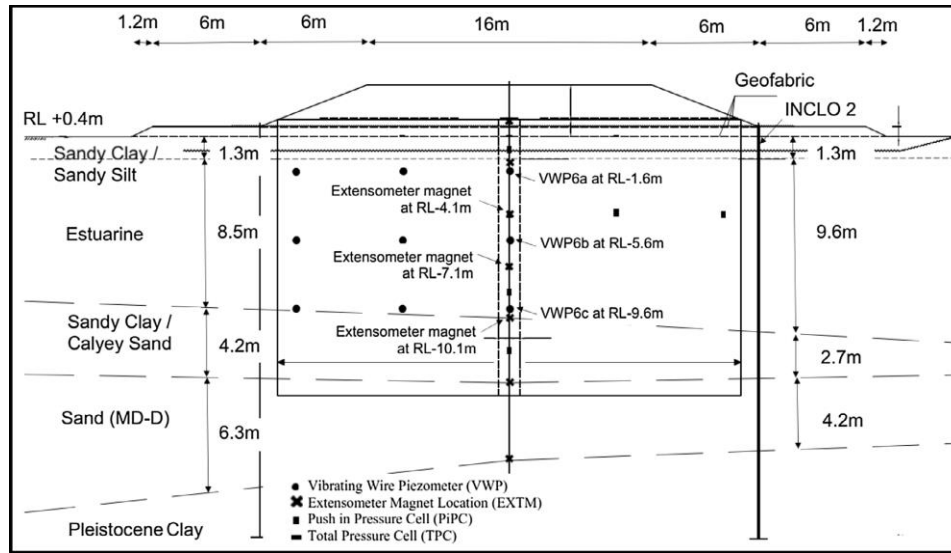


Figure 1. Geotechnical section of the instrumented trial embankment (Chan, Poon, and Perera 2018)

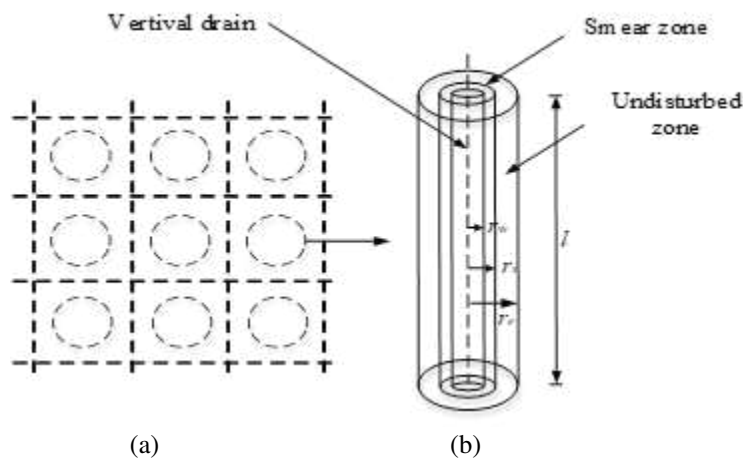


Figure 2. Vertical drain installation pattern and unit cell.

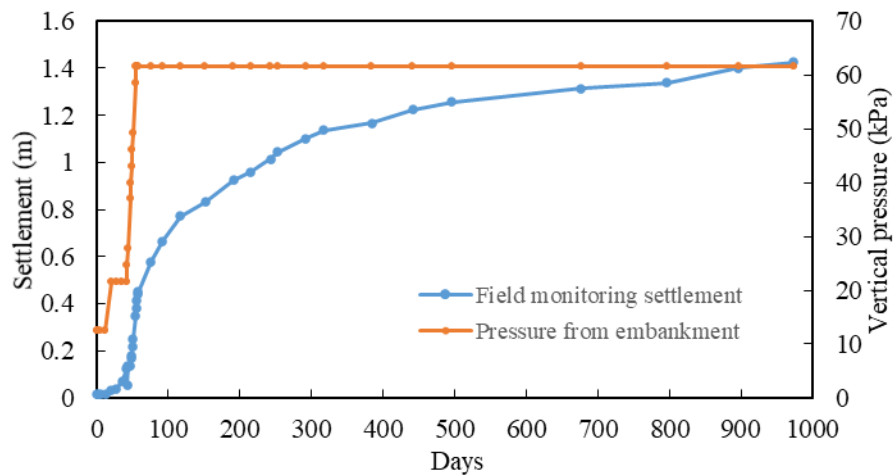


Fig. 3. Field monitoring settlement and embankment loading history



PREDICTION METHODS

The Asaoka Method

The Asaoka method is proposed by Asaoka (1978) to predict the ultimate settlement of a single uniform soil layer in-situ and the coefficient of consolidation for one-dimensional consolidation with settlement data. This method is actually a graphical procedure to estimate the ultimate settlement by interpreting and extrapolating field observations of settlement. According to the Asaoka method, the one-dimensional consolidation settlements ($\delta_0, \delta_1, \delta_2, \dots$) in equal time intervals ($0, \Delta t, 2\Delta t, \dots$) can be expressed as:

$$\delta_n = \beta_0 + \beta \delta_{n-1} \quad (1)$$

where β_0 is the intercept, β is the slope of the line, δ_n is the settlement at elapsed time t_n , δ_{n-1} is the settlement time t_{n-1} , and $t_n - t_{n-1}$ equals to a constant value Δt .

When the ultimate settlement δ_{ult} has been reached, we have:

$$\delta_n = \delta_{n-1} = \delta_{ult} \quad (2)$$

Therefore, δ_{ult} can be obtained by determining the intersection point between the Asaoka plot (δ_{n-1} vs. δ_n) and the line $\delta_n = \delta_{n-1}$. The Terzaghi theory settlement is used for the time increment ΔT_v of 0.01, 0.025, and 0.05. These are plotted in the Asaoka form of δ_{n-1} vs. δ_n , and are presented in Fig.4.

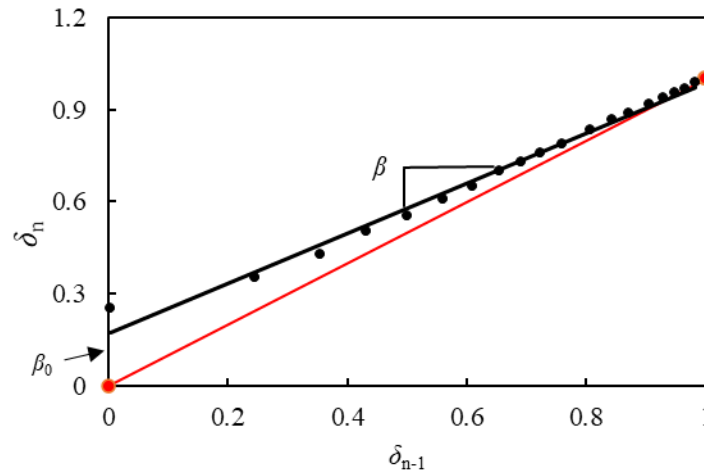


Figure 4. Asaoka plots for the Terzaghi theory for $\Delta T_v = 0.05$ (Tan and Chew 1996).

The Hyperbolic Method

The Hyperbolic method was proposed and refined by Tan et al. (1993, 1994, 1995) for obtaining the coefficient of consolidation c_v from odometer tests. The Hyperbolic method is particularly useful in the field for one single isotropic soil layer. Once some data are available and it's observed that the behavior is following a hyperbolic pattern, the subsequent consolidation can be then predicted. According to Sridharan and Rao (1981), the Terzaghi theory of consolidation gives a unique settlement-time plot in terms of the average degree of consolidation against the time factor, U_v vs. T_v .

A plot of T_v / U_v versus T_v obtained from the Terzaghi consolidation theory is also shown in Fig.5(a), where $T_v = c_v t / H^2$ and H is the maximum vertical drainage distance. The curve is initially concave downward, followed by an approximately linear segment which corresponds to the range of $60\% < U_v < 90\%$ (Sridharan, Murthy, and Prakash 1987). According to Tan (1993), the linear segment of the theoretical hyperbolic curve can be taken to start at $U_v = 50\%$ and is described by:

$$\frac{T_v}{U_v} = \alpha_i T_v + \beta \quad (3)$$



where α_i is the theoretical slope of the initial linear segment between the 60% and 90% consolidation stages; α_i equals to 0.821 (Tan and Chew 1996), which is a unique value applicable only to Terzaghi's theory; and β is the intercept of the Hyperbolic plot on the T_v / U_v axis.

The field settlement data are plotted in the form of t / δ vs. t in Fig.5(b). According to Tan (1971), Kodandaramaswamy and Rao (1980), and Narasimha (1981), the relationship between settlement δ and time t is assumed to follow a hyperbolic curve given by the equation:

$$\frac{t}{\delta - \delta_0} = \beta + S_i t \quad (4)$$

where t is the time from the start of applying the hyperbolic function after the end of embanking, δ is the settlement at time t , δ_0 is the settlement when t equals to 0, and S_i and β are the slope and the intercept of the straight line, respectively.

Based on Eq. (4), the hyperbolic plot of t / δ versus time t is a straight line and the ultimate settlement can be obtained by:

$$\lim_{t \rightarrow \infty} \delta = \lim_{t \rightarrow \infty} \frac{1}{\beta + S_i} + \delta_0 = \frac{1}{S_i} + \delta_0 \quad (5)$$

Eq. (5) is applicable for the prediction at the early consolidation stage. However, Sridharan and Rao (1981), Sridharan, Murthy, and Prakash (1987), and Tan (1993, 1994) indicated that the relationship between the field settlement δ and time t does not fit a rigorous straight line. Therefore, the ultimate settlement cannot always be determined from Eq. (5). Tan (1994) thus proposed that reasonable prediction of ultimate settlement can be obtained by the product of the inverse of the slope of the initial linear portion of the hyperbolic plot fitted to actual settlement data, $1 / S_i$, and the slope of the initial linear portion of the theoretical hyperbolic curve, α_i .

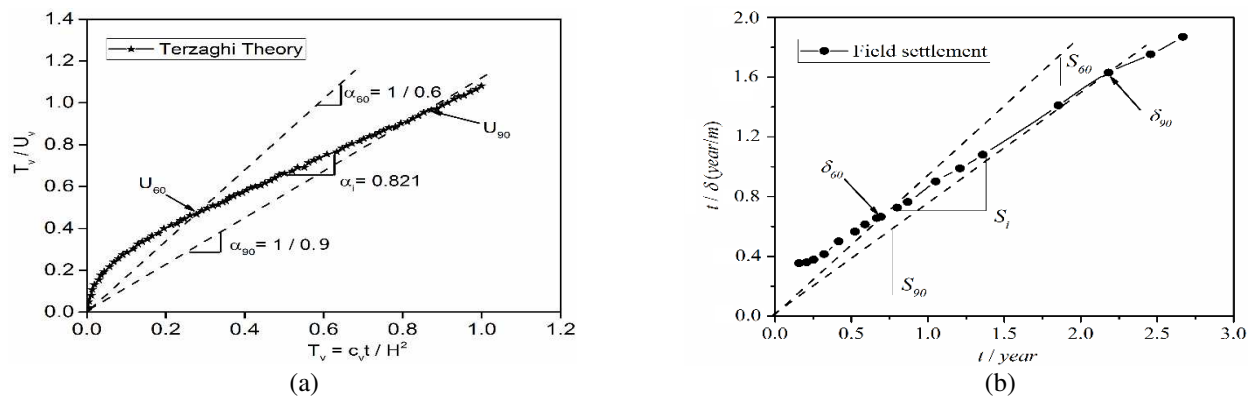


Figure 5. Hyperbolic plots of the Terzaghi theory and field settlement data.

As presented in Fig.5(a), the slopes S_{60} and S_{90} can be determined by the relationships that the slopes of lines radiating from the origin to S_{60} and S_{90} consolidation points make with the linear segment of the plots, which can be represented as:

$$S_{60} = S_i \frac{\alpha_{60}}{\alpha_i} \quad (6)$$

$$S_{90} = S_i \frac{\alpha_{90}}{\alpha_i} \quad (7)$$

As the 60% and 90% consolidation points can be easily determined by constructing radiating lines from the origin to intersect the first linear segment of the field hyperbolic plot, the ultimate settlement can then be estimated as $\delta_{60} / 0.6$ or $\delta_{90} / 0.9$, where δ_{60} and δ_{90} are 60% and 90% of the ultimate settlement, respectively. Therefore, the line radiating from the origin to the 60% settlement point in the Fig.5(b) can be expressed by:

$$\frac{t}{\delta} = \frac{1}{0.6} \frac{S_i}{\alpha_i} \quad (8)$$



In Fig.5(b), t_{60} is the time and δ_{60} is the settlement at the 60% consolidation stage. Thus, δ_{60} can be obtained from Eq. (8) as:

$$\delta_{60} = \frac{t_{60}}{\left(\frac{t_{60}}{\delta_{60}}\right)} = \frac{1}{0.6} \frac{\alpha_i}{S_i} \quad (9)$$

Thus, the ultimate settlement $\delta_{60}/0.6$ is simply α_i/S_i . Similarly, it can be extended for the 90% consolidation point. Therefore, the ultimate settlement δ_{ult} can be calculated with three different ways by:

$$\delta_{ult} = \frac{\alpha_i}{S_i} = \frac{\delta_{60}}{0.6} = \frac{\delta_{90}}{0.9} \quad (10)$$

The Bayesian Method

Considering the uncertainties associated with input soil properties and monitored data, the parameters need to be updated and the new monitored information should be combined into the updating process consistently, which is best tackled as a Bayesian statistical inference problem. In this study, the Bayesian theorem and a Markov chain Monte Carlo (MCMC) algorithm are adopted to update the parameters. Based on the updated parameters, the numerical consolidation analyses of the Ballina multi-layered embankment soil profile subjected to a series of loading sequences are carried out using a forward marching finite difference procedure.

Probabilistic Parameter Updating

Several sources of errors, such as uncertainties associated with the input soil properties and the monitored data, should be rationally considered and incorporated into predictions. It is important to quantify the uncertainties in predicted values in order to be prepared for appropriate action if the predicted values turn out to be significantly lower or higher than the expected values. Considering the uncertainties existing in some of the soil parameters, those uncertain parameters are thus modeled as random variables x . A measurement error e is defined as the difference between the actual performance d and the model prediction $F(x)$. We then have:

$$d = F(x) + e \quad (11)$$

Based on the Bayesian theorem, the posterior information is inferred by updating prior probability distribution with monitored data. This process can be expressed with:

$$P(x|d) = cL(x|d)P(x) \quad (12)$$

where c is a normalized constant and $L(x|d)$ is the likelihood function. $P(x)$ is the prior distribution reflecting the knowledge about x prior to obtaining the field-monitored data. The prior information is usually obtained from site investigation, engineering judgement, and experience. The posterior information $P(x|d)$ is obtained by updating x , which incorporates both the prior information and the field monitored behaviors.

Likelihood Function

The likelihood function includes the mechanical model to relate the observations to the model parameters x . It also presents the difference between the measurements d_i and the predictions $F_i(x)$, which is caused by the measurement errors e_i —something to follow a zero-mean Gaussian distribution and which can be modeled explicitly through PDF $f_e()$. The likelihood is proportional to the probability of observing the behavior for a given value of x , and it is given as:

$$L_i(x|d_i) = \frac{1}{(2\pi)^{\frac{N_d}{2}} \det(R_i)^{\frac{1}{2}}} \times \exp\left\{-\frac{1}{2}[d_i - F_i(x)]^T R_i^{-1}[d_i - F_i(x)]\right\} \quad (13)$$

where N_d is the number of points in a specific type of the observation, i represents the number of types of monitored behavior, And R_i is the coefficient of variation (COV) of the measurement error corresponding to the monitored data and can be represented by:

$$R_i = \begin{bmatrix} \sigma_{i,1}^2 & 0 & \cdots & 0 \\ 0 & \sigma_{i,1}^2 & \cdots & 0 \\ \vdots & \vdots & \ddots & \vdots \\ 0 & 0 & \cdots & \sigma_{i,N_d}^2 \end{bmatrix} \quad (14)$$



where $\sigma_{i,j} = COV_{i,err} \times d_{i,j}$ and $COV_{i,err}$ is the coefficient of variation (COV) of the measurement error corresponding to the monitored data $d_{i,j}$ ($j = 1, 2, \dots, N_d$).

Markov Chain Monte Carlo (MCMC) Algorithm

The posterior distributions should be derived through sampling methods. The basic idea of MCMC simulation is that of drawing samples from an arbitrary distribution and then correcting those samples to better approximate and finally converge to the target posterior distribution. The Markov chain Monte Carlo (MCMC) method is particularly popular as it allows direct sampling from posterior distribution without the need to evaluate a potentially high dimension integral in the Bayesian formulation. In this study, the posterior non-linear high dimension distributions are obtained by efficient multi-chain MCMC simulations using DREAM(ZS)(Vrugt et al. 2008; Laloy and Vrugt 2012).

THE BALLINA EMBANKMENT SETTLEMENT PREDICTION

Settlement Prediction Using the Asaoka Method

Based on field measurement data as shown in Fig.6, different time increments Δt (10, 20, 50, and 100 days) and settlement data monitored in different periods (0 to 200 days and 0 to 1,000 days) are adopted to study the influence of the time increment and consolidation stage on the accuracy of this method. The obtained results are presented in Fig. 6, where the round point is the field monitored settlement data and the slope is β ; the red line represents the settlement data obtained by the least squares linear regression method; the black solid line represents $\delta_n = \delta_{n+1}$, and the slope is 1. δ_{ult} is the predicted ultimate settlement.

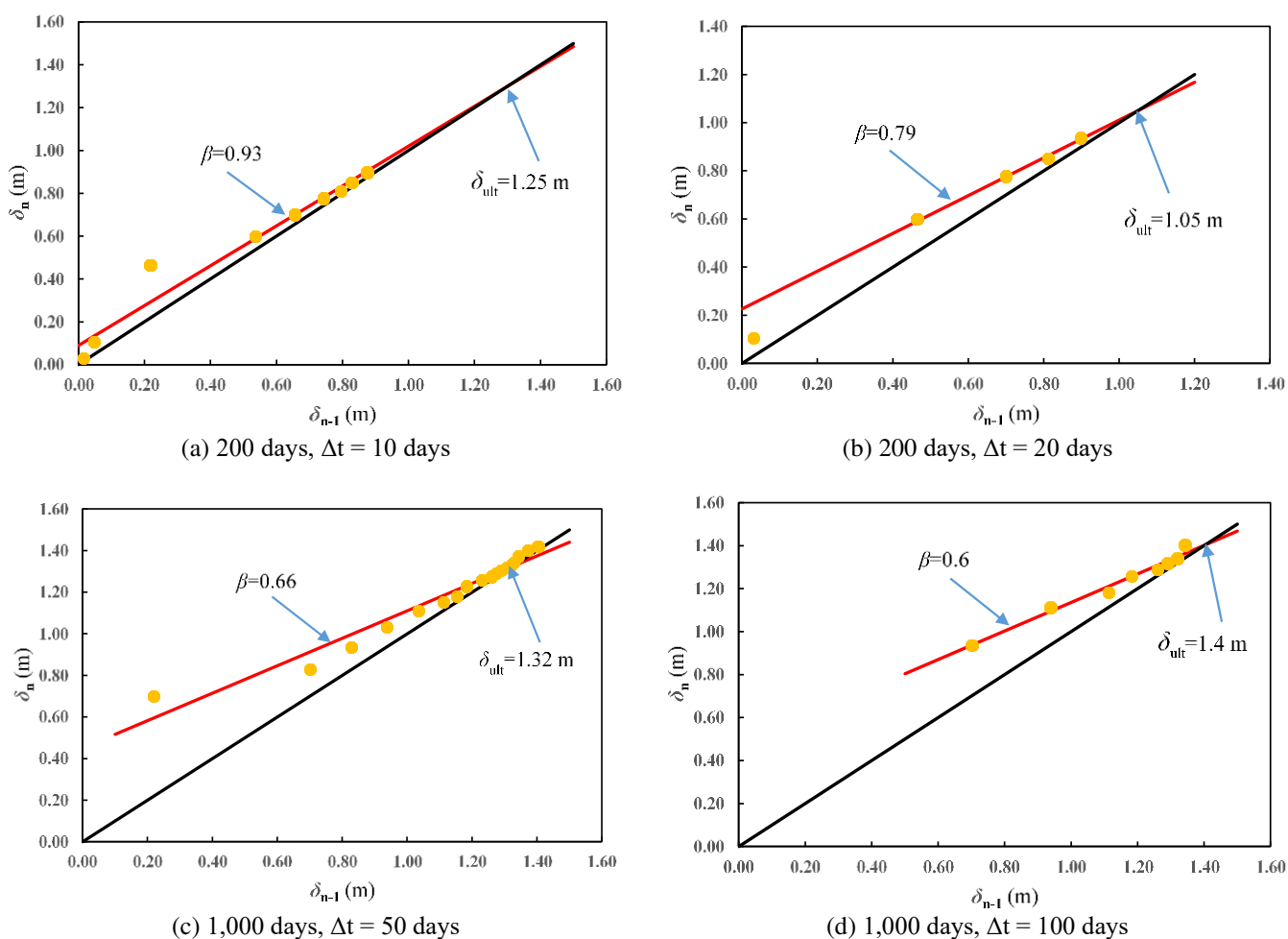


Figure 6. Results of the Asaoka method.



As shown in Fig.6, based on 200 days of settlement data, the ultimate settlements predicted by the Asaoka method using 10-day and 20-day increments are 1.25 m and 1.05 m, respectively, which provide very low estimates of δ_{ult} . Using 1,000 days of settlement data, the Asaoka method predicted ultimate settlements of 1.40 m and 1.32 m when 100-day and 50-day increments are applied respectively. These predictions are closer to the actual settlement than when using 200 days of data. It can be concluded that a good prediction can only be obtained when settlement data of a higher degree consolidation stage is incorporated and a larger time increment is employed.

Settlement Prediction Using the Hyperbolic Method

The settlement data cannot be used in the Hyperbolic method if the filling is not completed in a short period of time, as the rate of filling is not constant. According to the loading history of the Ballina embankment, which is presented in Fig.3, the filling was completed in 58 days and the settlement was 0.45 m. The settlement data beyond 58 days are plotted in Fig.7 and Fig.8, based on the measurements before 215 days and 974 days, respectively.

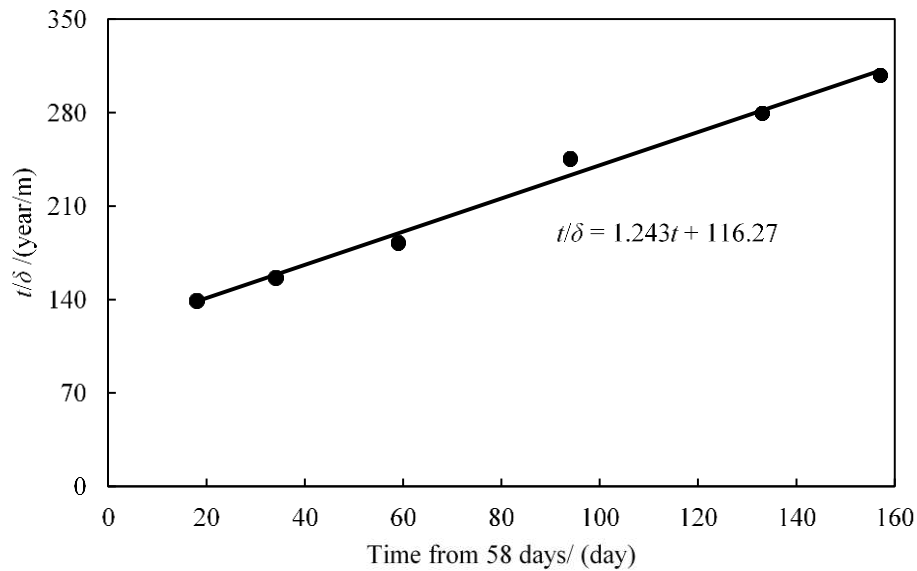


Figure 7. Results of the Hyperbolic method based on the measurements prior to 215 days.

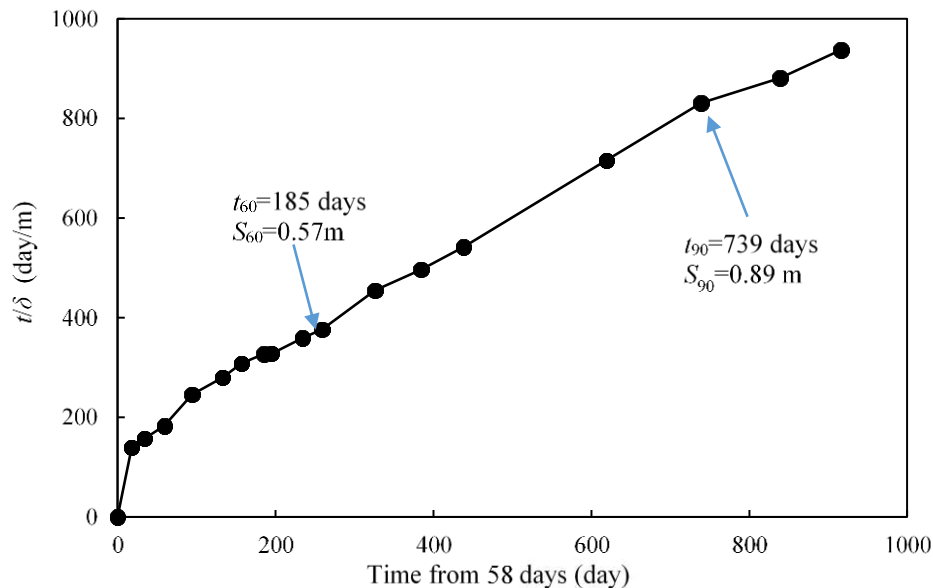


Figure 8. Results of the Hyperbolic method based on the measurements before 974 days.



It can be seen from Fig.7 that the slope of the linear segment $S_i = 1.243$, and the predicted ultimate settlement δ_{ult} is $1 / S_i + S_0 = 1 / 1.243 + 0.45 = 1.255$ m.

In Fig.8, the ultimate settlements δ_{ult} predicted by the Hyperbolic method are $\delta_{60} / 0.6 + S_0 = 0.57 / 0.6 + 0.45 = 1.4$ m and $\delta_{90} / 0.9 + S_0 = 0.89 / 0.9 + 0.45 = 1.44$ m, based on t_{60} and t_{90} respectively. The slope S_i , based on Fig.8, is $S_i = 0.8897$. The ultimate settlement δ_{ult} can also be estimated as $0.821 / 0.8897 + 0.45 = 1.373$ m. All three estimates of the final settlement based on the Hyperbolic method are similar.

Settlement Prediction Using the Bayesian Method

Model Description

In this study, the consolidation settlement is calculated by a forward marching finite difference procedure. The modified Cam-Clay model (Roscoe and Burland 1968; Roscoe, Schofield, and Thurairajah 1963) is implemented in this procedure to calculate the ultimate embankment settlement. In accordance with the site investigation, the soil profile under the Ballina embankment is divided into nine layers, as shown in Fig. 9. For one-dimensional consolidation finite difference analyses, the soil layers are divided by the nodes, which are located at the top and base of each layer and are equally spaced in between, as indicated in Fig. 9, where I is the index of the node point. The number of divisions of each layer adopted in this study is presented in Table 1, and Δ_n represents the thickness of the n th division in Fig. 9.

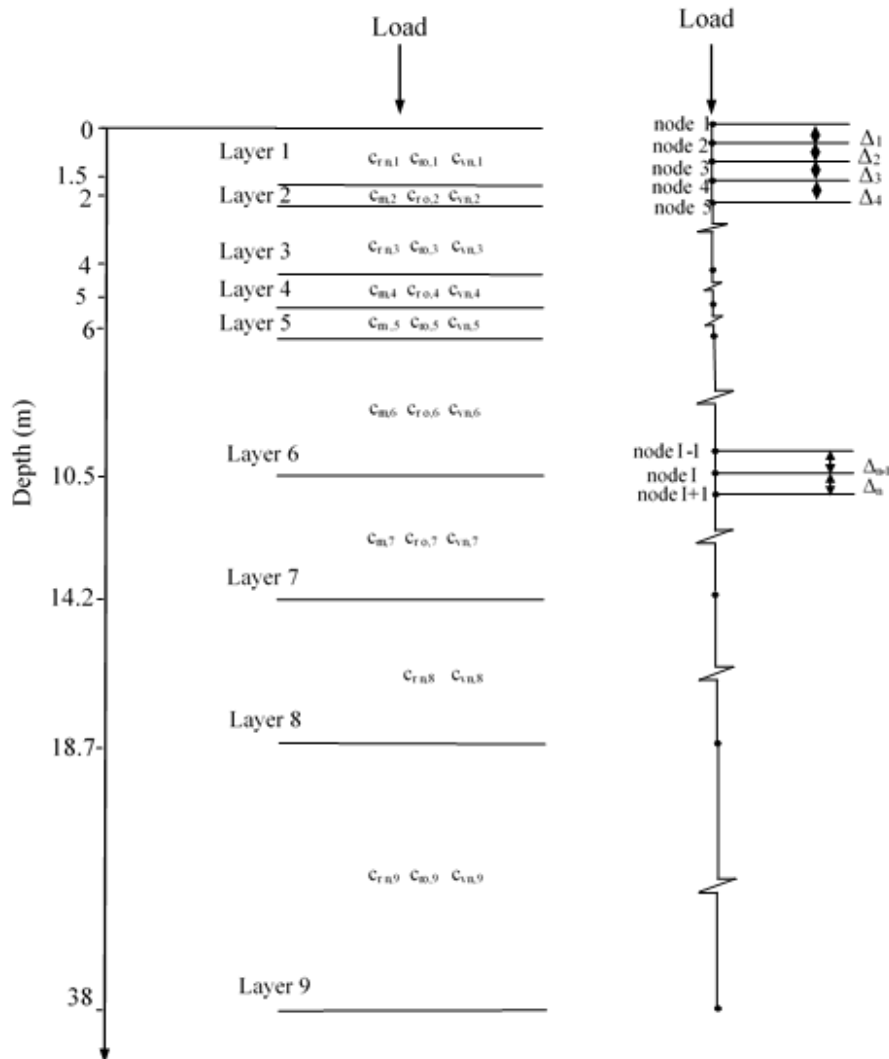


Figure 9. Soil profile, random variables in soil layers, and the definition of the node point of the instrumented trial embankment.



Two sets of value, the compression ratio c_r and the coefficient of consolidation c_v , need to be input for each layer. In Fig. 9, $c_{rn}(j)$ and $c_{vn}(j)$ represent c_r and c_v values for the soil in a normally consolidated state, and $c_{ro}(j)$ and $c_{vo}(j)$ are the values for the soil in an over-consolidated state, respectively, where j represents the number of the soil layer. In this study, $c_{vo}(j)$ is assumed as $0.1 c_{vn}(j)$, and the values of $c_{ro}(j)$ and $c_{vo}(j)$ for Layer 8 (the sand layer) are considered to be unchanged during the updating process. To reflect the rate-effect in the constant rate of strain (CRS) odometer test, a factor α is introduced to multiply the pre-consolidation pressure (σ'_p). In total, there are thus 27 random variables (26 soil parameters and 1 factor α) that are considered as random variables x in Eq. (11). The 26 soil parameters are considered as log-normally distributed to avoid negative values. The factor α is deemed to be uniformly distributed with a range of 0.6-1.0 in this study. CRS odometer tests show that the over consolidation ratio (OCR) generally ranges from 1.2 to 2.2.

Shown in Table 1 are the adopted prior statistics of the soil parameters for nine soil layers, the pre-consolidation stress σ'_p , the coefficient of consolidation in an over-consolidated state (c_{vo}), the slope of unloading-reloading line (κ), and the initial void ratio (e_0) according to the laboratory test and prior literature by Kelly et al. (2018); Zheng et al. (2018). The mean and the standard deviation of the measured settlement error are considered as 0 and 0.02 m, respectively (Kelly and Huang 2015b).

According to the data collected by site investigation and geotechnical tests, the initial and final depths of the water table below the surface are both 1.5 m. The unit weight of water is $9.81 \text{ kN} / \text{m}^3$. PVDs are installed in a rectangular pattern, as shown in Fig. 2, and are thus modeled by equivalent axisymmetric unit cells. Fig. 2(b) shows a unit cell with an external radius r_e and an initial one-way drainage path length l . The equivalent radii of the vertical drain, smear zone, and undistributed zone are $r_w = 25 \text{ mm}$, $r_s = 0.125 \text{ m}$, and $r_e = 0.677 \text{ m}$, respectively, in this study. Darcy's law for fluid flow is assumed to be valid.

Table 1. Statistics of prior distributions

| Layer | Soil | Depth (m) | No. of divisions | σ'_p (kPa) | c_m | c_{ro} | c_{vn} | c_{vo} | e_0 | κ | COV [c_m, c_{ro}] | COV [c_{vn}] |
|-------|--------------------|-----------|------------------|-------------------|-------|----------|----------|----------|-------|----------|-----------------------|------------------|
| 1 | Crust | 0-1.5 | 3 | 35.5 | 0.055 | 0.017 | 0.411 | 4.11 | 0.81 | 0.013 | 0.3 | 3 |
| 2 | Clay | 1.5-2 | 1 | 65.3 | 0.304 | 0.024 | 0.016 | 0.164 | 1.63 | 0.028 | 0.3 | 3 |
| 3 | Clay | 2-4 | 4 | 53.5 | 0.408 | 0.042 | 0.016 | 0.164 | 2.31 | 0.061 | 0.3 | 3 |
| 4 | Clay | 4-5 | 2 | 70.3 | 0.721 | 0.048 | 0.005 | 0.055 | 3.16 | 0.087 | 0.3 | 3 |
| 5 | Clay | 5-6 | 2 | 71.9 | 0.540 | 0.051 | 0.005 | 0.055 | 2.89 | 0.087 | 0.3 | 3 |
| 6 | Clay | 6-10.5 | 9 | 85 | 0.582 | 0.059 | 0.005 | 0.055 | 3.19 | 0.107 | 0.3 | 3 |
| 7 | Transition to sand | 10.5-14.2 | 8 | 80.2 | 0.589 | 0.118 | 0.005 | 0.055 | 0.7 | 0.087 | 0.3 | 3 |
| 8 | Sand | 14.2-18.7 | 9 | 1000 | 0.187 | 0.013 | 0.86 | 8.6 | 0.6 | 0.009 | 0.3 | 3 |
| 9 | | 18.7-38 | 40 | 350 | 0.536 | 0.077 | 0.005 | 0.055 | 0.4 | 0.047 | 0.3 | 3 |

Predicted Settlement

Back analysis is conducted starting at a period from 0 to 36 days to update the soil parameters. Based on the monitoring settlement of the surface of the embankment during 0 to 36 days, prior information, and the Bayesian updating approach, the MCMC samples of the posterior distributions of the parameter x are generated. The updated parameters are then used to predict the settlement of surface after 36 days. The process is repeated until the end. The predicted settlement at the ground surface using data from 0 to 36 days is denoted with the legend "36 d" in Fig.10 and the same meaning of "36 d" can be extended to the legend "51 d", "71 d", "117 d", ..., "974 d". In Fig.10, the monitored data is represented by circles with a measurement and prior prediction which are obtained by exclusively using prior information, which is denoted by a dashed line. The posterior mean values of the soil properties based on the Bayesian updating scheme using monitored data from 0 to 36 days, 51 days, ..., 974 days are presented in Table 2.

As presented in Fig.10, the predicted settlement can converge to the corresponding monitored data by incorporating more field measurements into the Bayesian updating process. For example, the prediction using monitored settlement from the 76th day, which is better than the prior prediction, still deviates from the monitored data. When using data prior to the 215th day, however, the prediction of the ground surface settlement is in better agreement with the monitored data. The discrepancy



between the predicted and observed settlement, using data prior to the 215th day, is around 0.09 m and relatively small. This result is much better than that prior to Bayesian updating and predicting.

Table 2. Mean values of updated soil parameters using various days of monitored settlement

| Soil properties | Soil layer | Variable number | Prior | 36d | 51d | 76d | 117d | 215d | 292d | 384d | 496d | 797d | 974d |
|-----------------|------------|-----------------|-------|-------|-------|-------|-------|-------|-------|-------|-------|-------|-------|
| c_m | 1 | 1 | 0.055 | 0.013 | 0.061 | 0.073 | 0.063 | 0.07 | 0.061 | 0.058 | 0.061 | 0.085 | 0.059 |
| | 2 | 2 | 0.304 | 0.148 | 0.341 | 0.412 | 0.351 | 0.319 | 0.377 | 0.415 | 0.256 | 0.277 | 0.504 |
| | 3 | 3 | 0.408 | 0.433 | 0.513 | 0.698 | 0.624 | 0.659 | 0.693 | 0.641 | 0.634 | 0.685 | 0.72 |
| | 4 | 4 | 0.721 | 0.889 | 0.648 | 0.732 | 0.743 | 0.702 | 0.656 | 0.634 | 0.672 | 0.413 | 0.219 |
| | 5 | 5 | 0.540 | 0.663 | 0.52 | 0.565 | 0.617 | 0.6 | 0.677 | 0.653 | 0.589 | 0.172 | 0.66 |
| | 6 | 6 | 0.582 | 0.404 | 0.684 | 0.34 | 0.16 | 0.308 | 0.603 | 0.756 | 0.34 | 0.94 | 0.471 |
| | 7 | 7 | 0.589 | 0.552 | 0.627 | 0.557 | 0.798 | 0.718 | 0.726 | 0.527 | 0.801 | 0.656 | 0.71 |
| | 8 | 8 | 0.187 | 0.128 | 0.172 | 0.216 | 0.171 | 0.2 | 0.217 | 0.18 | 0.154 | 0.307 | 0.349 |
| | 9 | 9 | 0.536 | 0.308 | 0.502 | 0.595 | 0.52 | 0.57 | 0.54 | 0.391 | 0.488 | 0.423 | 0.803 |
| c_{ro} | 1 | 10 | 0.017 | 0.007 | 0.017 | 0.012 | 0.013 | 0.015 | 0.015 | 0.012 | 0.016 | 0.006 | 0.008 |
| | 2 | 11 | 0.024 | 0.032 | 0.025 | 0.025 | 0.022 | 0.03 | 0.024 | 0.019 | 0.027 | 0.043 | 0.016 |
| | 3 | 12 | 0.042 | 0.058 | 0.041 | 0.036 | 0.041 | 0.034 | 0.033 | 0.038 | 0.044 | 0.012 | 0.01 |
| | 4 | 13 | 0.048 | 0.44 | 0.043 | 0.045 | 0.055 | 0.054 | 0.043 | 0.048 | 0.043 | 0.103 | 0.062 |
| | 5 | 14 | 0.051 | 0.054 | 0.053 | 0.061 | 0.044 | 0.038 | 0.034 | 0.042 | 0.047 | 0.041 | 0.024 |
| | 6 | 15 | 0.059 | 0.028 | 0.065 | 0.083 | 0.06 | 0.071 | 0.052 | 0.07 | 0.061 | 0.045 | 0.013 |
| | 7 | 16 | 0.118 | 0.113 | 0.115 | 0.12 | 0.097 | 0.122 | 0.094 | 0.11 | 0.129 | 0.212 | 0.144 |
| | 8 | 17 | 0.013 | 0.014 | 0.013 | 0.013 | 0.011 | 0.012 | 0.014 | 0.014 | 0.01 | 0.015 | 0.01 |
| | 9 | 18 | 0.077 | 0.052 | 0.072 | 0.078 | 0.063 | 0.069 | 0.067 | 0.078 | 0.098 | 0.089 | 0.103 |
| c_{vn} | 1 | 19 | 0.411 | 0.353 | 0.113 | 0.588 | 0.357 | 0.487 | 0.604 | 0.755 | 0.251 | 0.743 | 0.707 |
| | 2 | 20 | 0.016 | 0.035 | 0.012 | 0.005 | 0.002 | 0.005 | 0.003 | 0.004 | 0.004 | 0.147 | 0.119 |
| | 3 | 21 | 0.016 | 0.067 | 0.048 | 0.141 | 0.105 | 0.141 | 0.15 | 0.151 | 0.15 | 0.148 | 0.148 |
| | 4 | 22 | 0.005 | 0.014 | 0.011 | 0.01 | 0.001 | 0.004 | 0.003 | 0.001 | 0.003 | 0.02 | 0.039 |
| | 5 | 23 | 0.005 | 0.014 | 0.004 | 0.006 | 0.003 | 0.002 | 0.001 | 0.001 | 0.002 | 0.016 | 0.01 |
| | 6 | 24 | 0.005 | 0.027 | 0.004 | 0.016 | 0.011 | 0.014 | 0.009 | 0.007 | 0.01 | 0.009 | 0.015 |
| | 7 | 25 | 0.005 | 0.026 | 0.01 | 0.001 | 0.015 | 0.003 | 0.001 | 0.001 | 0.001 | 0.004 | 0.003 |
| | 8 | 26 | 0.005 | 0.026 | 0.004 | 0.002 | 0.004 | 0.003 | 0.009 | 0.002 | 0.004 | 0.009 | 0.041 |
| | α | | 27 | 1 | 0.93 | 0.843 | 1.143 | 1.057 | 1.096 | 1.048 | 1.041 | 0.97 | 1.205 |

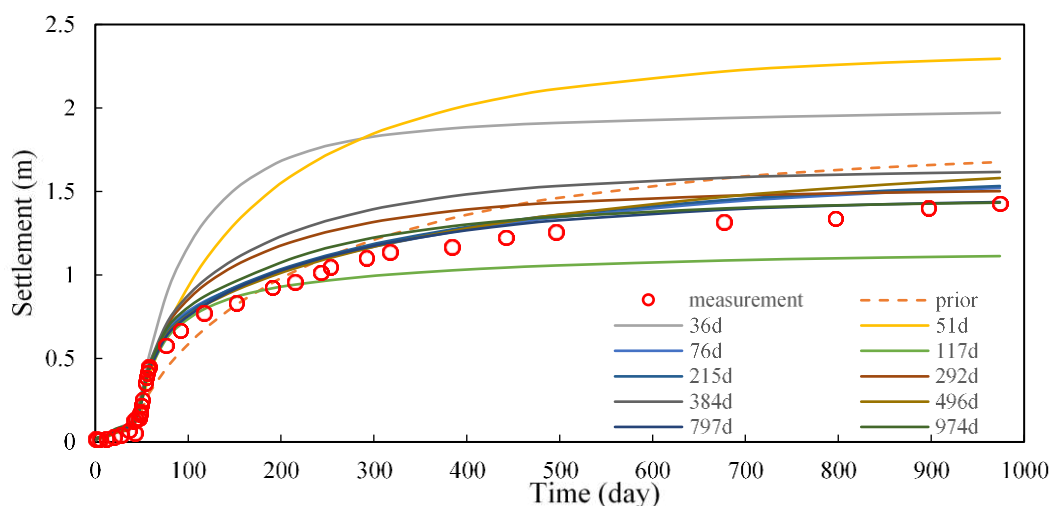


Figure 10. Predicted settlement at surface using different numbers of monitored settlements



COMPARISON ANALYSES

In this section, the predicted ultimate settlement using three different methods and the different amount of monitoring data is summarized in Table 3. t_{90} , for instance, represents the settlement predicted using the Hyperbolic method based on a 90% consolidation stage.

Table 3. The predicted ultimate settlement using three different methods (m).

| Days of Settlement Data (Day) | Asaoka Method | | | | Hyperbolic Method | | Bayesian Approach | | Measurements |
|-------------------------------|------------------|------|------|------|-------------------------------|-------------------------------|-------------------------------|-------------------------------|--------------|
| | Δt (day) | | | | Days of Settlement Data (Day) | Predicted Ultimate Settlement | Days of Settlement Data (Day) | Predicted Ultimate Settlement | |
| 10 | 20 | 50 | 100 | | | | | | |
| 200 | 1.25 | 1.05 | - | - | 215 | 1.255 | 215 | 1.531 | 1.429 |
| 1000 | - | - | 1.32 | 1.40 | 974 (t_{90}) | 1.44 | 797 | 1.434 | |

According to Table 3, the three methods provide similar results, and the accuracy of the predicted results can be improved if more measurement data is incorporated. Both of the settlement predictions found by the Hyperbolic method (using 974 days' worth of settlement data) and the Bayesian method (using settlement data prior to the 797th day) are in agreement with the monitoring field data. The predicted settlement based on the Bayesian approach using settlement data prior to the 215th day, where the average consolidation degree is 52.12%, is quite close to the field ultimate settlement

CONCLUSIONS

This study successfully applied the Asaoka method, the Hyperbolic method, and the Bayesian approach to estimate the ultimate settlement of the Ballina embankment. The following conclusions are obtained:

1. The accuracy of the predicted settlement by the three methods would be improved if more monitoring data was incorporated.
2. The Asaoka and Hyperbolic methods can provide a good prediction of the ultimate settlement in many cases. Limitations still exist in the usage of both of these methods, since they can only be applied to one single isotropic soil layer, and settlement data beyond the 60% consolidation stage is needed to make accurate predictions of the ultimate settlement.
3. Regarding the Asaoka method, the selection of a time increment, which depends on designers, can significantly influence the accuracy of the settlement prediction.
4. For settlements predicted by the Hyperbolic method, the determination of the 60% and 90% consolidation points is subject to practitioners, which indicates that the accuracy of this method cannot be guaranteed.
5. The Bayesian approach can be applied to settlement predictions for multi-layered soils. It only takes 215 days of settlement data to gain quite a reliable prediction of future settlements. That means future settlement can be confidently estimated by the Bayesian approach at an early stage, which is essential to achieve cost-effective outcomes and helps eliminate additional earthworks during construction and/or avoid the risk of post-construction performance not meeting the project criteria.

ACKNOWLEDGEMENTS

This research was funded by the Australian Government through the Australian Research Council, the Chinese Government through the China Scholarship Council, and the University of Newcastle through CSC top-up scholarship.

REFERENCES

- Asaoka, A. (1978). "Observational procedure of settlement prediction." *Soils and foundations*, 18(4), 87-101.
- Buttling, S., Cao, R., Lau, W., and Naicker, D. (2018). "Class A and Class C numerical predictions of the deformation of an embankment on soft ground." *Computers and Geotechnics*, 93, 191-203.



-
- Chan, K.F., Poon, B.M., and Perera, D. (2018). "Prediction of embankment performance using numerical analyses—Practitioner's approach." *Computers and Geotechnics*, 93, 163-77.
- Honjo, Y., Wen-Tsung, L., and Guha, S. (1994). "Inverse analysis of an embankment on soft clay by extended Bayesian method." *International Journal for Numerical and Analytical Methods in Geomechanics*, 18(10), 709-34.
- Hsein, J.C., Luo, Z., Atamturktur, S., and Hongwei, H. (2013). "Bayesian updating of soil parameters for braced excavations using field observations." *Journal of Geotechnical and Geoenvironmental Engineering*, 139, 395-406.
- Kelly, R.B., Sloan, S.W., Pineda, J.A., Kouretzis, G., and Huang, J. (2018). "Outcomes of the Newcastle symposium for the prediction of embankment behaviour on soft soil." *Computers and Geotechnics*, 93, 9-41.
- Kelly, R.B., Pineda, J.A., Bates, L., Suwal, L.P., and Fitzallen, A. (2017). "Site characterisation for the Ballina field testing facility." *Géotechnique*, 67(4), 279-300.
- Kelly, R.B., and Huang, J. (2015a). "Bayesian updating for one-dimensional consolidation measurements." *Canadian Geotechnical Journal*, 52(9), 1318-30.
- Kelly, R.B., and Huang, J. (2015b). "Bayesian updating for one-dimensional consolidation measurements." *Canadian Geotechnical Journal*, 52, 1318-30.
- Kodandaramaswamy, K., and Rao, S.N. (1980). "The prediction of settlements and heave in clays." *Canadian Geotechnical Journal*, 17, 623-31.
- Laloy, E., and Vrugt, J.A. (2012). "High-dimensional posterior exploration of hydrologic models using multiple-try DREAM (ZS) and high-performance computing." *Water Resources Research*, 48(1).
- Le, T., Airey, D., and Surjadinata, J. (2018). "Modelling the behaviour of the Ballina test embankment". *Computers and Geotechnics*, 93, 115-122.
- Lim, G.T., Pineda, J.A., Boukpeti, N., and Carraro, J.A.H. (2018). "Predicted and measured behaviour of an embankment on PVD-improved Ballina clay." *Computers and Geotechnics*, 93, 204-221.
- Liu, Z., Choi, J.C., Lacasse, S., and Nadim, F. (2018). "Uncertainty analyses of time-dependent behaviour of Ballina test embankment." *Computers and Geotechnics*, 93, 133-149.
- Miranda, T., Correia, A.G., and e Sousa, L.R. (2009). "Bayesian methodology for updating geomechanical parameters and uncertainty quantification." *International Journal of Rock Mechanics and Mining Sciences*, 46(7), 1144-1153.
- Müthing, N., Zhao, C., Hölter, R., and Schanz, T. (2018). "Settlement prediction for an embankment on soft clay." *Computers and Geotechnics*, 93, 87-103.
- Narasimha, R. (1981). "Proposed hyperbolic relationship between settlement and time."
- Pineda, J.A., Suwal, L.P., Kelly, R.B., Bates, L., and Sloan, S.W. (2016). "Geotechnical characterization of Ballina clay." *Géotechnique*, 66(7), 556-77.
- Rezania, M., Nguyen, H., Zanganeh, H., and Taiebat, M. (2018). "Numerical analysis of Ballina test embankment on a soft structured clay foundation." *Computers and Geotechnics*, 93, 61-74.
- Roscoe, K.H., and Burland, J.B. (1968). "On the generalized stress-strain behavior of wet clay".
- Roscoe, K.H., Schofield, A., and Thurairajah, A. (1963). "Yielding of clays in states wetter than critical." *Geotechnique*, 13(3), 211-40.
- Sridharan, A., Murthy, N.S., and Prakash, K. (1987). "Rectangular hyperbola method of consolidation analysis." *Geotechnique*, 37, 355-68.
- Sridharan, A., and Rao, A.S. (1981). "Rectangular hyperbola fitting method for one dimensional consolidation." *Geotechnical Testing Journal*, 4(4), 161-168.
- Tan, S.A. (1993). "Ultimate settlement by hyperbolic plot for clays with vertical drains." *Journal of geotechnical engineering*, 119(5), 950-6.
- Tan, S.A. (1994). "Hyperbolic method for settlements in clays with vertical drains." *Canadian Geotechnical Journal*, 31, 125-31.
- Tan, S.A. (1995). "Validation of hyperbolic method for settlement in clays with vertical drains." *Soils and Foundations*, 35(1), 101-113.
- Tan, S.A., and Chew, S. (1996). "Comparison of the hyperbolic and Asaoka observational method of monitoring consolidation with vertical drains." *Soils and Foundations*, 36, 31-42.
- Tan, S.B. (1971). "An empirical method for estimating secondary and total settlement." *Proc. 4th Asian Regional Conference on Soil Mechanics and Foundation Engineering*, Bangkok, 2, 147-51.
- Tan, T.S., Inoue, T., and Lee, S.L. (1991). "Hyperbolic method for consolidation analysis." *Journal of geotechnical engineering*, 117(11), 1723-1737.
- Tschuchnigg, F., and Schweiger, H.F. (2018). "Embankment prediction and back analysis by means of 2D and 3D finite element analyses." *Computers and Geotechnics*, 93, 104-114.
-



-
- Vrugt, J.A, Ter Braak, C.J.F., Diks, C.G., Hyman, J.M., Robinson, B.A., and Higdon, D. (2008). "Accelerating Markov chain Monte Carlo simulation by differential evolution with self-adaptive randomized subspace sampling." *International journal of nonlinear sciences and numerical simulation*, 10(3), 273-290.
- Yang, C., and Carter, J.P. (2018). "1-D finite strain consolidation analysis based on isotach plasticity: Class A and Class C predictions of the Ballina embankment." *Computers and Geotechnics*, 93, 42-60.
- Zhang, J, Tang, W., and Zhang, L. (2010). "Efficient probabilistic back-analysis of slope stability model parameters." *Journal of Geotechnical and Geoenvironmental Engineering*, 136(1), 99-109.
- Zheng, D., Huang, J., Li, D., Kelly, R.B., and Sloan, S.W. (2018). "Embankment prediction using testing data and monitored behaviour: A Bayesian updating approach." *Computers and Geotechnics*, 93, 150-162.



INTERNATIONAL JOURNAL OF GEOENGINEERING CASE HISTORIES

*The Journal's Open Access Mission is
generously supported by the following Organizations:*



Access the content of the *ISSMGE International Journal of Geoengineering Case Histories* at:
www.geocasehistoriesjournal.org